Microstructural Characterization of Cross-Linkable *p*-Phenylene Terephthalamide–Terephthalic Acid Derivative (PPTA-*co*-XTA) Copolymer Fibers

M.-C. G. Jones, T. Jiang, and D. C. Martin*

Department of Materials Science and Engineering, The University of Michigan, Ann Arbor, Michigan 48109-2136

Received May 26, 1994; Revised Manuscript Received July 26, 1994•

ABSTRACT: We are studying the microstructure of PPTA-*co*-XTA copolymer fibers. XTA is a variant of terephthalic acid (TA) with a benzocyclobutene (BCB) cross-linking moiety which becomes reactive above the synthesis and processing temperatures but below the degradation temperature. The fibers were dry-jet wet spun from lyotropic liquid crystalline solutions and heat-treated at various temperatures to induce structural reorganization and cross-linking. The microstructure was examined by wide-angle X-ray diffraction and molecular modeling. The copolymers retain the ability to crystallize and form well-oriented fibers. The BCB units are accommodated by a gradual increase in the distance between hydrogen-bonded sheets, the *a* dimension of the two-chain unit cell. The BCB units of high XTA content copolymers segregate into (100) planes. The *a*, *b*, and *c* dimensions of the unit cell of un-cross-linked PPXTA are respectively 0.91, 0.47, and 1.24 nm. Cross-linking does not significantly change the diffraction patterns, suggesting that the reaction may occur preferentially within the grain boundaries between crystallites.

Introduction

Extended-chain organic fibers such as poly(*p*-phenylene terephthalamide) (PPTA) are composed of long macromolecules virtually completely oriented parallel to the fiber axis. This leads to an extremely high tensile modulus (≈200 GPa) and tensile strength (≈4 GPa). However, these fibers have a number of problems including weakness in compression, relatively poor adhesion in composite matrices, environmentally accelerated creep, and low abrasion resistance.[1]

Failure of oriented polymeric fibers in compression occurs by strain localization within kink bands. The plastic deformation within kink bands results from the low intermolecular shear strength which allows sliding between molecules.[2] The creep of Kevlar 29 and 49 has been attributed to crystallite rotation, leading to an improvement of orientation.[3] A recent model explains creep in oriented polymers by the transport and annihilation of conformational defects along the polymer chain.[4]

Incorporating interchain covalent cross-links has the potential to improve both the behavior in compression and during creep. Interchain cross-links should prevent to some degree the sliding between molecules and should slow the transport of conformational defects. By increasing the concentration of lateral covalent bonds, the material would evolve from an anisotropic array of stiff molecules to a more isotropic, three-dimensional network.

Various schemes for cross-linking extended-chain polymers have been presented. Sweeny's approach was based on the thermal elimination of an activated aryl halogen, followed by combination of the aryl free radicals thus formed, leading to ring coupling.[5] Poly[*p*-phenylenebenzobisthiazole] fiber compressive strength was found to improve with cross-linking. However, other properties such as tensile strength, tensile modulus and toughness were reduced.

Rickert et al. synthesized the 2,2,6,6-tetraoxo-1,3,5,7-tetrahydro-2,6-dithia-*s*-indacene-4,8-diamine (DSDA).[6]

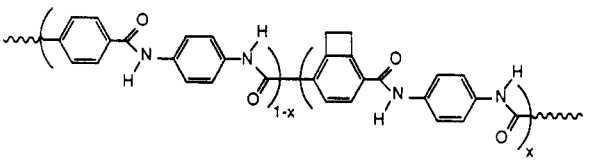

Figure 1. Chemical structure of PPTA-*co*-XTA copolymers.

DSDA is a reactive derivative of *p*-phenylenediamine and undergoes a thermal ring-opening reaction at about 330 °C, with SO_2 release and generation of the reactive *o*-quinodimethane intermediate. PPTA-*co*-DSDA fibers were studied, for which the DSDA is "sleeping" during synthesis and processing and cross-links in the post-spin heat treatment. Only copolymers containing up to 20 mol % DSDA relative to the total diamine content were soluble in sulfuric acid and could be spun into fiber. The compressive strength and torsional modulus were found to decrease with increased DSDA content. The tensile strength and modulus were lowest for the copolymer containing 20 mol % DSDA relative to the total diamine content.[7]

A family of monomers was designed specifically as reactive derivatives of terephthalic acid (TA) so that they may be incorporated into many types of extended-chain polymers.[8] One of these new monomers, XTA, contains the thermally activated cross-linking agent benzocyclobutene (BCB). The BCB ring opens at elevated temperature to form the reactive *o*-quinodimethane intermediate.[9] We are studying PPTA-*co*-XTA copolymer fibers.[10,11] The reactive monomer is used as a comonomer incorporated within the backbone of the extended chains and may be thermally activated during a post-spinning heat treatment. The BCB units cross-link in the solid state at about 380 °C, with no volatile formation. This is above the polymer synthesis and processing temperatures (≈100 °C) but below the degradation temperature (≈500 °C). A schematic representation of PPTA-*co*-XTA copolymers is illustrated in Figure 1.

The microstructure of PPTA-*co*-XTA copolymer fibers of low XTA content is expected to be similar to that of PPTA fibers. PPTA fibers (Kevlar) have been the object

• Abstract published in *Advance ACS Abstracts*, September 1, 1994.

0024-9297/94/2227-6507$04.50/0

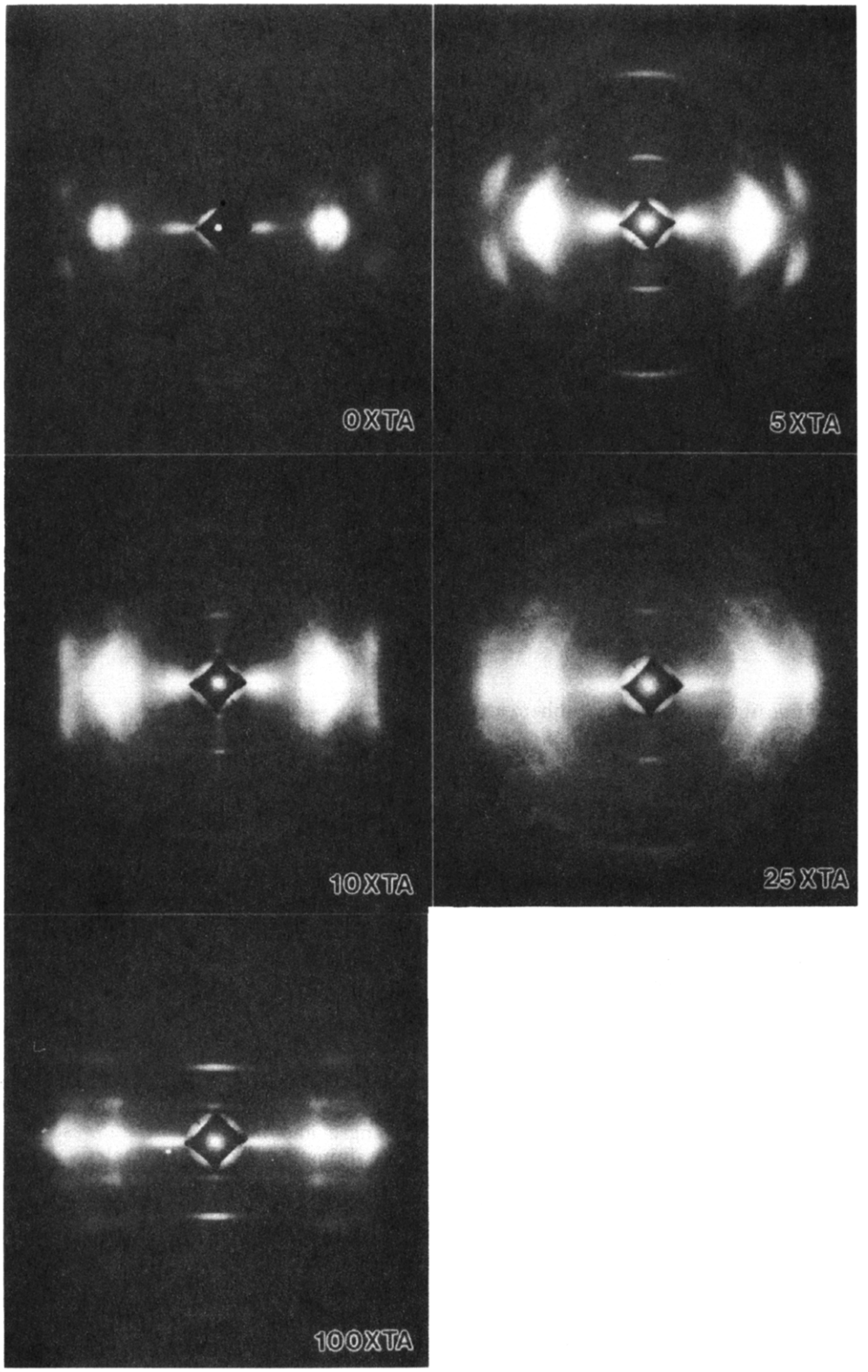

Figure 2. WAXD of fibers of various XTA content heat-treated at 260 °C.

of numerous studies.[12-15] The solid state structure consists of highly oriented crystalline domains. Two crystal structures have been identified. Both have a monoclinic unit cell (pseudo-orthorhombic) with two chains per unit cell. The chain axis is assigned parallel to the c direction. The chains intersect the ab plane at [0,0] and [$^1/_2$,$^1/_2$] in the "Northolt" or base-centered structure[12] and [0,0] and [$^1/_2$,0] in the "Haraguchi" or edge-centered structure.[13] In both cases the unit cell dimensions are approximately: a = 0.8 nm, b = 0.5 nm, and c = 1.3 nm. Along the direction of the b-axis the chains are laterally associated by hydrogen bonds, while weaker secondary interactions exist in other directions normal to the chain axis.

The hydrogen-bonding interactions in the (100) planes lead to the association of PPTA chains into sheets.[14] Within the same sheet the hydrogen bonds between chains are relatively strong and have very specific directions. On the other hand, the secondary bonds between chains in neighboring sheets are weaker and nondirectional. The resulting lack of preferred registry between sheets is consistent with the existence of the two polymorphs that have been observed experimentally. Several crystalline

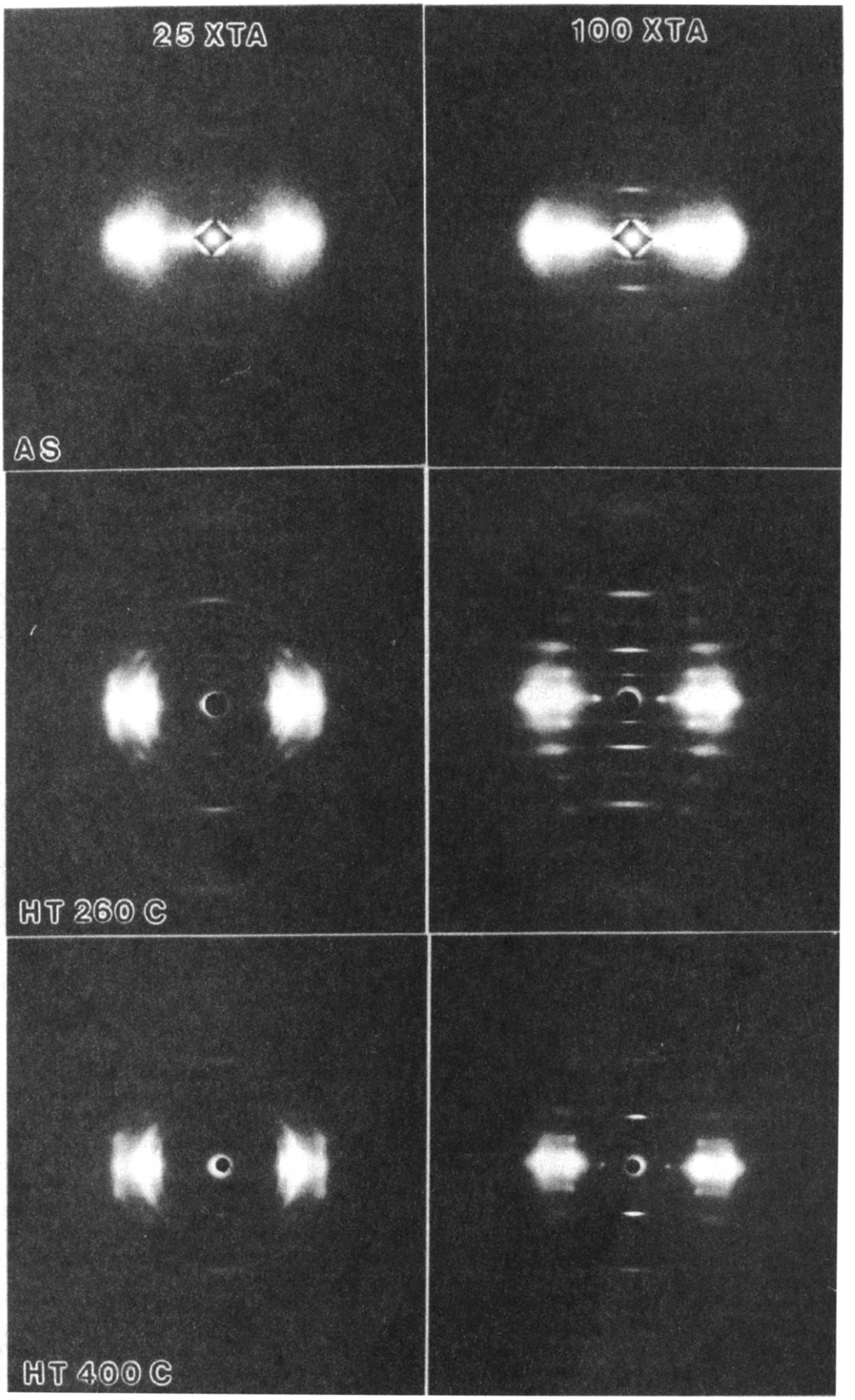

Figure 3. WAXD of PPTA-*co*-25XTA and PPXTA, as spun, HT 260 °C, and HT 400 °C. Notice the (001) and (100) reflections for PPXTA.

polymorphs of comparable stability have been found in modeling studies.[16]

We present here a study of the microstructure of the PPTA-*co*-XTA copolymers before and after cross-linking. These copolymers contain 5, 10, 25, and 100% XTA relative to the total diacid content.

Experimental Procedures

Materials and Heat Treatment. The synthesis of the PPTA-*co*-XTA polymers has been described elsewhere.[10,11] XTA contains the benzocyclobutene (BCB) moiety and was designed to be a reactive derivative of terephthalic acid used in the synthesis of PPTA molecules.[8] Similarly to the PPTA polymer, these

copolymers can form a nematic liquid crystalline solution when dissolved into sulfuric acid. The processing of the copolymers into well-oriented fibers using the dry-jet wet spinning techniques has been previously described.[17]

The fibers studied are PPTA-*co*-5XTA, PPTA-*co*-10XTA, PPTA-*co*-25XTA, and PPXTA (or PPTA-*co*-100XTA) fibers, in their as-spun and tension heat-treated (260 or 400 °C) states. Typically a tension heat treatment of organic fibers is performed to improve the crystallinity. In the case of our reactive copolymers, the BCB unit is thermally activated at about 380 °C; the materials heat-treated at 400 °C are therefore cross-linked. This was confirmed by swelling experiments.[18]

Microstructural Characterization. X-ray Diffraction. Wide-angle X-ray diffraction (WAXD) experiments were performed at The University of Michigan and at Wright Patterson Air Force Base on flat-film cameras with pinhole collimation. The radiation generated at The University of Michigan was from a Philips X-ray unit with a Fe target (0.194 nm) and a Mn filter. The X-ray source at Wright Patterson Air Force Base was Cu Kα radiation (0.154 nm) from a Rigaku RU-300 or RU-200 rotating-anode generator with a graphite crystal as the monochromator. Each fiber specimen was wound along the fiber axis to form a bundle that was attached vertically onto the exit of the collimator. A Si or a Ni standard was used for calibration. The camera length was typically 3 cm.

Molecular Modeling of Un-Cross-Linked PPXTA. Simulations of the crystal structure of PPXTA were done with POLYGRAF and CERIUS software of Molecular Simulations Inc. using the Dreiding II force field. The intramolecular force field contains contributions from bond stretching, valence angle bending, torsional, and inversion terms. Nonbonded interactions include van der Waals, electrostatic, and hydrogen-bonded terms. Periodic boundary conditions were used. As for PPTA, there are two chains per unit cell.

The molecules were first built in CERIUS and then the energy was minimized in POLYGRAF using the Dreiding II force field with the default settings. CERIUS was used to monitor the energy as a function of shifting between hydrogen-bonded sheets, along the *b* and *c* directions. The second chain positioned roughly at $^1/_2a$ was first brought to a (*b*,*c*) = (0,0) position, equivalent to the position of the first chain (a = 0) but in the nearby hydrogen-bonded plane. This was done by translation in the *b* (hydrogen bond direction) and *c* (molecular axis direction) directions. Then the second chain was translated along *b* and *c* directions and the energy recorded. Energy maps were then plotted, keeping the individual chain conformations and the unit cell parameters unchanged. For energy minima of interest the structure was minimized in POLYGRAF and the theoretical diffraction pattern calculated with CERIUS.

Results and Discussion

WAXD Analysis. Figure 2 shows the WAXD patterns of the various copolymer fibers tension heat-treated at 260 °C. The diffraction patterns exhibit systematic variations with XTA content. The copolymers of 10% or less XTA have diffraction patterns similar to that of PPTA. However, the fibers of 25% or more XTA exhibit noticeably different reflections. Thus, the addition of BCB units leads not necessarily to enhanced lattice distortion but to a new packing geometry. This was not observed for the PPTA-*co*-DSDA fibers studied by Glomm et al., presumably because of the low DSDA content (20% or less).[7] The authors only reported a small difference in the observed *d*-spacings of the copolymers compared to those of PPTA.

The WAXD patterns of as-spun, heat-treated at 260 °C and heat-treated at 400 °C (e.g., cross-linked) materials are presented for PPXTA and PPTA-*co*-25XTA in Figure 3. The fiber diffraction patterns contain meridional and equatorial reflections indicative of the anisotropy. The as-spun fibers are well oriented as a result of the spinning processes.[17] Heat treatment of the as-spun fibers leads to improved molecular ordering and orientation. In addition, the heat-treated fibers exhibit well-defined off-axis reflections, revealing the development of three-dimensional order during heat treatment.

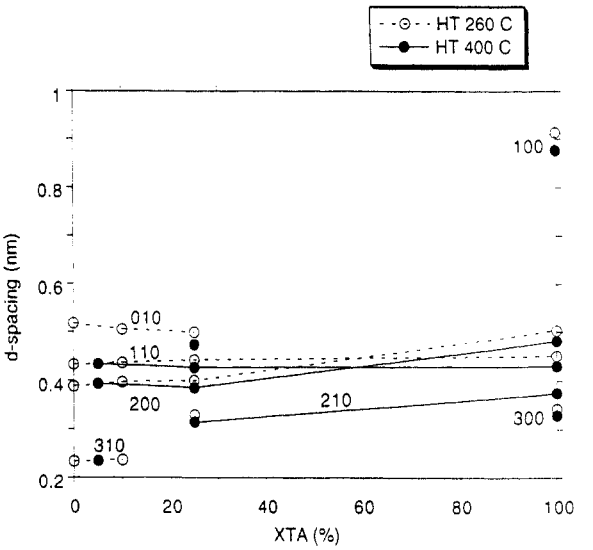

Figure 4. Plot of *d*-spacings versus XTA content.

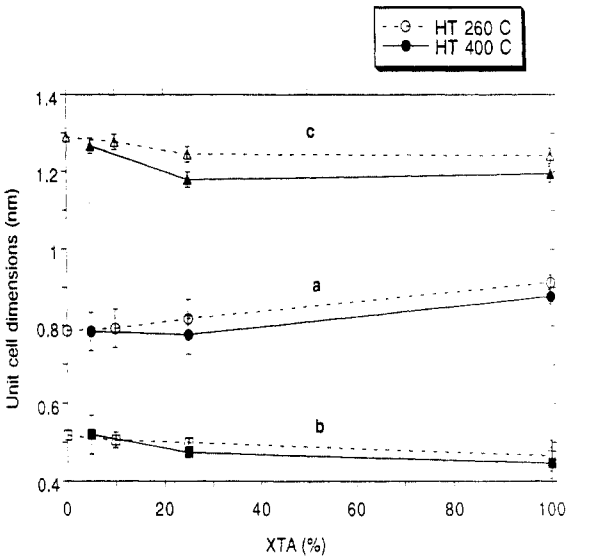

Figure 5. Plot of the *a*, *b*, and *c* dimensions of the two-chain unit cell versus XTA content.

The diffraction patterns of fibers tension heat-treated at 260 and 400 °C appear similar. One could have expected some loss of chain orientation as reported by Glomm et al.[7] In fact the cross-linking reaction neither induces misorientation nor disrupts the order. Whether there is competition between structural reorganization and cross-linking reaction during the 400 °C heat treatment or the cross-linking reaction occurs after some structural reorganization has been done, cross-linking does not hinder or disrupt the order.

One could also have expected the development of a new "cross-linked" crystal structure with the appearance of additional reflections in the diffraction pattern of the fibers tension heat-treated at 400 °C. As mentioned, however, the diffraction patterns of un-cross-linked or cross-linked fibers are not dramatically different. The lack of a well-defined diffraction signature in the cross-linked system suggests that the cross-linking reaction may occur not within the crystalline phase but in the less ordered grain-boundary areas between crystallites.

WAXD Indexing. Figure 4 is a plot of the *d*-spacings versus XTA content observed in the WAXD patterns of the PPTA-*co*-XTA copolymer fibers, as a function of the

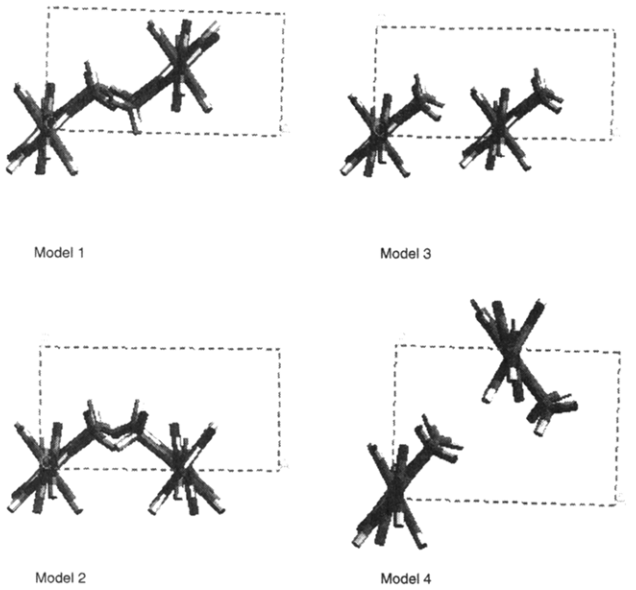

Figure 6. Four different geometrical possibilities for the unit cell of PPXTA. The XTA units are parallel for models 1 and 3 and perpendicular for models 2 and 4.

identified diffracting planes. The suggested indexing scheme requires a nonprimitive unit cell with two chains per unit cell. The structures of other extended-chain polymers such as PPTA[12] and poly[*p*-phenylenebenzobisoxazole][19] are also described by a two-chain unit cell. The concept of unit cell in this study is not that of a periodic repeat unit in a classically perfect crystalline material. The unit cells used for oriented organic fibers correspond to an average unit cell of paracrystalline domains. In fact the unit cell dimensions as well as the exact atomic positions vary statistically from cell to cell.[20] For the case of copolymers it is still possible to define an average unit cell with some variation of the molecular content from cell to cell. The origin of three-dimensional order has been previously studied in an oriented assembly of randomly sequenced chains, more specifically in wholly aromatic liquid crystalline copolymers.[21–25] Two different models of order have been proposed, namely, the nonperiodic layer model of Windle et al.[21] and the paracrystalline lattice model of Biswas and Blackwell.[22–25]

In their PPTA-*co*-DSDA copolymers, Glomm et al. suggested a transition from a Haraguchi type structure to a Northolt type structure upon heat treatment.[7] Haraguchi previously reported such a transformation when annealing PPTA films coagulated in water;[13] the transformation was found significant for films prepared from sulfuric acid solutions of low polymer concentrations. In our case, the as-spun fibers are not sufficiently ordered to make possible an unambiguous indexing of the pattern to any particular polymorph.

The diffraction reflections along the meridian correspond to (00*l*) planes and give information about the sequence distribution along the chain backbone and the axial misregistry between the chains. In the case of PPTA-*co*-XTA materials, the axial misregistry is likely to arise mostly from the shifting between hydrogen-bonded planes. The (001) reflection is weak in the diffraction pattern of PPTA because of the symmetry of the unit cell. Examination of the diffraction patterns in Figures 2 and 3 shows that the (001) reflection becomes stronger with increasing XTA content. For the homopolymer PPXTA consisting of alternating XTA and diamine phenylene rings, the axial

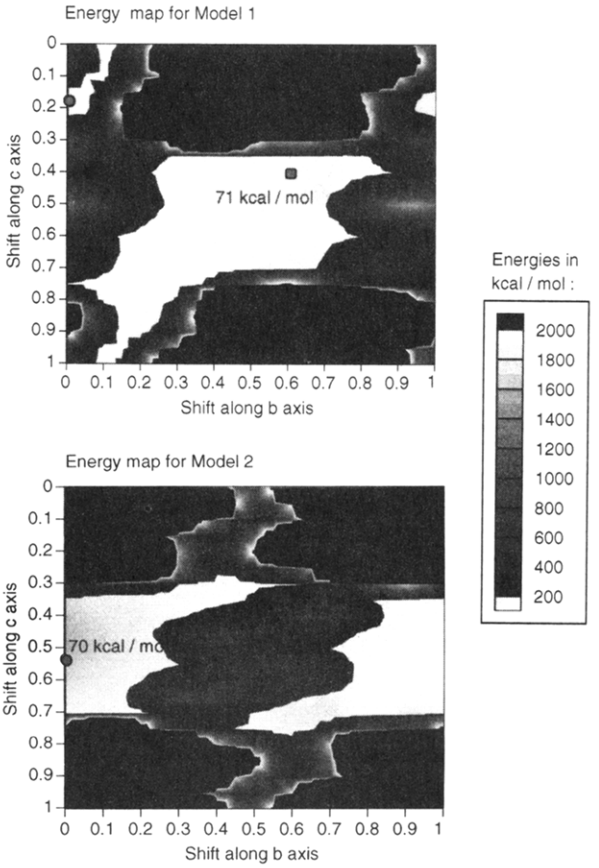

Figure 7. Energy maps for *y* and *z* translations between hydrogen-bonded sheets of PPXTA, for models 1 and 2.

misregistry dictates the intensities of the meridional reflections. The weaker intensity of (001) compared to that of (002) implies that the axial shift between the hydrogen-bonded sheets is closer to 50% than to no axial shift.

The equatorial diffraction reflections corresponding to (*hk*0) planes are determined by the lateral packing between chains. A Hull and Davey chart may be used to find the possible indexing scheme for an orthorhombic unit cell.[20] The reflections of PPXTA are indexed as follows: (100), (200) and (110), (210), (300), (310). This corresponds to a ratio of the unit cell dimensions b/a of approximately 0.51. The diffracting equatorial planes are (010), (110), (200), and (310) for PPTA-*co*-5XTA and PPTA-*co*-10XTA. For PPTA-*co*-25XTA the indexing scheme is (010), (110) and (200), (210) which corresponds to a b/a ratio of approximately 0.61. A plot of the *a*, *b*, and *c* dimensions as a function of XTA content is shown on Figure 5. The presence of a (110) reflection for all the PPXA-*co*-XTA copolymers suggests that the copolymers are predominantly of the Northolt type structure. Both the (110) and (200) reflections are distinguishable on the negatives of the diffraction patterns of PPXTA.

The size of the PPTA-*co*-XTA copolymer unit cell changes systematically with XTA content. The BCB groups are accommodated by an increase in the *a* direction which is the weakest secondary bond direction. The *b* and *c* unit cell dimensions do not vary much with composition. *b* is determined by the hydrogen bond length which is little disturbed by the introduction of the various amounts of BCB units. *c*, corresponding to the axial repeat unit, seems to decrease slightly with increasing XTA content. For their PPTA-*co*-DSDA copolymers, Glomm et al. did not report any increase in the distance between hydrogen-bonded planes with DSDA content.[7] It is likely

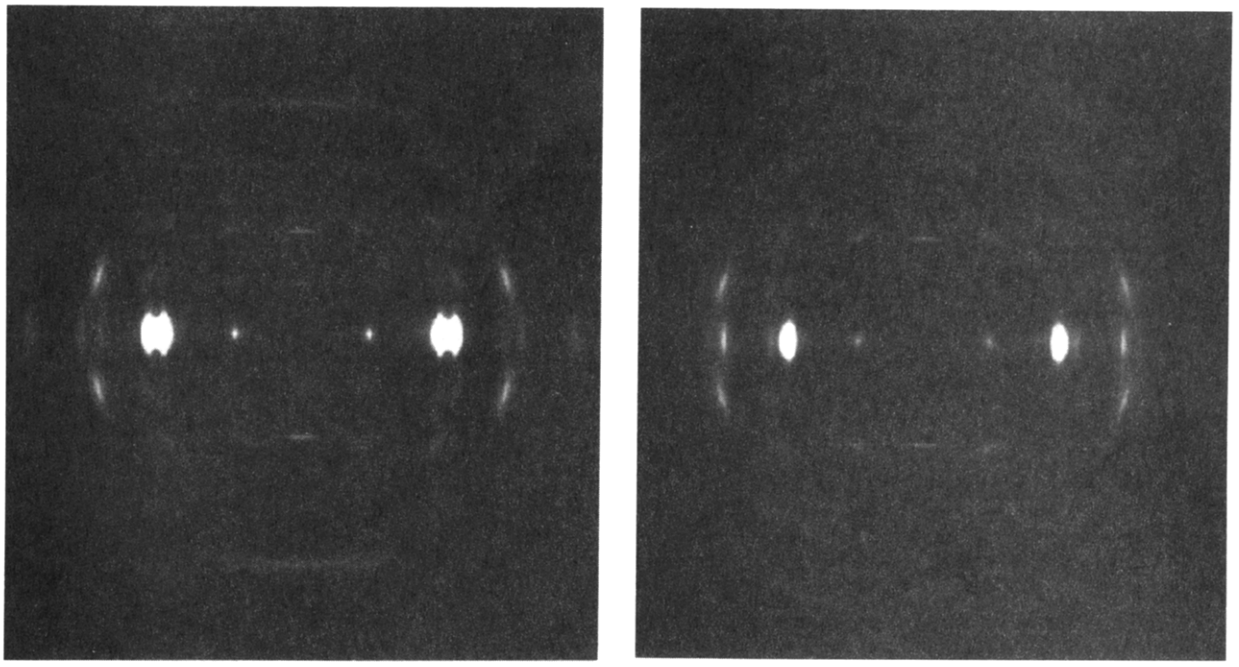

Figure 8. Simulated diffraction patterns of models 1 and 2.

that such an increase was not so apparent due to the maximum DSDA content of only 20 mol %.

Molecular Modeling of Un-Cross-Linked PPXTA. The (100) reflection in the PPXTA diffraction patterns exists in addition to the (200) reflection because the chains are not equidistant in the *a* direction. The implication is that the BCB units are neither unidirectional nor randomly oriented. The (100) reflection is not detected in the diffraction patterns of PPTA-*co*-25XTA, suggesting that the BCB units are randomly oriented in low XTA content copolymers.

There are four geometrical possibilities for the unit cell of PPXTA, two where the XTA units are parallel, either in the same direction or facing each other, and two where the XTA units are perpendicular. Figure 6 shows the four possible types of unit cells. Only models 1 and 2 with the BCB units segregated into (100) planes are consistent with the experimental data. For model 3, the (100) planes do not diffract. In model 4, the BCB groups interfere with one another such that the molecules are no longer hydrogen bonded in the *b* direction. The corresponding increase in the (010) spacing is not observed experimentally. Other low energy minima were found, but in all cases the (010) spacing is larger than observed experimentally.

The PPTA-*co*-XTA fibers therefore contain BCB-rich (100) planes alternating with BCB-poor (100) planes, as shown on models 1 and 2. It is reasonable to imagine that there will be occasional interruptions in the regularity of the (100) planes causing streaking on the layer lines of the PPXTA material. Indeed more streaking is observed on the layer lines of PPXTA than in the case of neat PPTA (Figure 2).

The energy maps for translations between hydrogen-bonded sheets of PPXTA are shown for models 1 and 2 in Figure 7. The energy minima are represented by circles. Model 1 corresponds to the lowest energy minima of two minima of energies 71 and 133 kcal/mol, separated by an energy height of 167 kcal/mol. The total energy of model 2 is similar to that of model 1: 70 kcal/mol. The structures of models 1 and 2 are respectively of the Northolt and Haraguchi type.

The theoretical diffraction patterns of models 1 and 2 are presented in Figure 8. Critical comparison of the calculated diffraction pattern of model 1 and of the experimental one in Figure 3 shows that the overall equatorial reflections are represented well, including the (100) reflection. However, the (300) reflection in the model is too weak. The (211) is stronger than observed experimentally. The overall meridional reflections are represented including the (004) reflection. The intensity of (002) is stronger than that of (001) as seen on the experimental data.

The major difference in the simulated diffraction patterns of models 1 and 2 resides in the intensity of the (110) reflection: strong for model 1 of the Northolt type structure but weak for model 2 of the Haraguchi type structure. Model 1 is therefore the best model since the (110) reflection is observed experimentally. In addition, model 1 is a better fit than model 2 to the meridional reflections. However, it is not possible to conclude definitively whether the PPXTA structure is only of the Northolt type structure. For PPTA it has been shown that either the Northolt or the Haraguchi structure may be preferentially induced by choosing appropriate processing parameters.[3] Our processing parameters were not particularly aimed at a specific crystal structure.

In conclusion the best unit cell is the one described by model 1, in which the BCB units are roughly coplanar and segregated into (100) planes. The position of the second chain is located at fractional coordinates of 0.57 along *a*, 0.55 along *b* which makes the structure more of the Northolt type, and 0.42 along *c*. The experimentally determined *a*, *b*, and *c* dimensions of the unit cell are respectively 0.91, 0.47, and 1.24 nm. The atomic coordinates of PPXTA for model 1 are available from the authors upon request.

Cross-Linking Reaction. Figure 9 shows possible schemes for cross-linking PPTA-*co*-XTA which are consistent with the suggestions of Marks[26] for BCB groups. Note that three out of four of the proposed reactions occur between two BCB units. However, copolymers of low XTA content have been cross-linked,[18] suggesting that the cross-

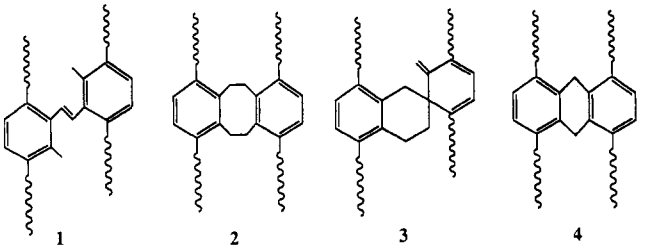

Figure 9. Possible schemes for cross-linking reactions. Reactions 1–3 occur between two BCB units. Reaction 4 occurs between a BCB unit and a phenylene ring.

link reaction does not require the proximity of two BCB units. Information about the cross-linking reaction is being pursued by solid-state ^{13}C NMR, Fourier transform IR, and Raman spectroscopy.

DSC experiments show that the cross-linking reaction occurs between 350 and 425 °C, with the maximum exotherm around 380 °C.[17] Thus a 400 °C heat treatment temperature was chosen as a compromise between maximum cross-linking efficiency and high-temperature degradation. The percentage of BCB units that may cross-link upon heat treatment, or the efficiency of the cross-linking reaction, was evaluated using the ratio of the reaction heat of the material to the reaction heat of the model compound.[17] The model compound XTA has the highest efficiency (assumed 100%) due to the ease of molecular mobility. The PPXTA powder structure has the lowest efficiency, presumably due to its disorganized and low density structure. Finally, the efficiency of the PPXTA fibers was found to be 70%, higher than that of the powder. This study emphasizes the importance of the local environment to the occurrence of the cross-linking reaction.

The above results show the need to investigate further the location of the cross-linking reaction. Swelling data and thermal studies show that cross-linking does occur.[17,18] The question is about the location of the cross-linking reaction, on various length scales. It is believed, for example, that cross-linking does not occur between the microfibrils. It has been suggested that the compressive failure mechanism is not the buckling of chains but the buckling of fibrils located beneath the outer fiber surface.[27,28] Since the buckling of fibrils also requires the buckling of several macromolecules, both issues should be addressed.

As discussed throughout the results, the precise nature and location of the cross-links are not yet known. The lack of a diffraction signature for the cross-linked system strongly suggests that cross-linking occurs mostly within the grain-boundary phase and not in the crystalline phase. It has been shown that cross-links in crystalline polyethylene take place in the noncrystalline phase at the lateral grain boundaries between crystallites.[29-31] Boundary creep through crystallite rotation has been proposed to account for the experimentally observed creep strain of Kevlar 29 and 49.[3] Cross-links within the grain-boundary area would limit shear at the inter-crystalline boundaries and therefore slow crystallite rotation.

Conclusions

We have studied the microstructure of thermally cross-linkable PPTA-co-XTA copolymers using X-ray diffraction and molecular modeling. The copolymers form well-oriented fibers as a result of the spinning process, regardless of their composition. A 260 °C heat treatment improves molecular order without triggering the cross-linking reaction. The cross-linking reaction taking place during the 400 °C heat treatment evidently does not involve misorientation of the material or loss of order.

The PPTA-co-XTA diffraction reflections are indexed to a two-chain unit cell. The BCB groups are accommodated in the unit cell by a gradual increase in the a dimension, from 0.79 nm for PPTA[12] to 0.91 nm for PPXTA through intermediate values for the copolymers. The introduction of the BCB units causes an increase in the intensity of the (001) and (100) diffraction reflections. The presence of a (100) reflection indicates that the BCB units segregate into (100) planes. The (110) reflection is visible in all the copolymers, indicating that the PPTA-co-XTA crystal structures are predominantly of the Northolt type. Model 1 is the structure best representative of PPXTA. The position of the second chain is located at fractional coordinates of 0.57 along a, 0.55 along b as for a Northolt type structure, and 0.42 along c. The experimentally determined a, b, and c dimensions of the PPXTA unit cell are respectively 0.91, 0.47, and 1.24 nm.

The cross-linking reaction upon tension heat treatment does not leave a well-defined diffraction signature, suggesting that cross-linking preferentially takes place in the more disordered grain-boundary phase between crystallites. We have done additional work to characterize the local microstructure with low-dose high-resolution electron microscopy. Details about the evolution of the crystallite size with heat treatment will allow us to study the competition taking place between molecular ordering, crystal growth, and the cross-linking reaction.

Acknowledgment. This research was supported by the U.S. Army Advanced Concept Technology Committee (DAAK6-92-K-0005). M.-C.G.J. thanks Wright Patterson Air Force Base for letting her use their flat-film X-ray camera. The authors are grateful to K. A. Walker, L. J. Markoski, G. A. Deeter, G. E. Spilman, and J. S. Moore for synthesizing the XTA monomer and the PPTA-co-XTA copolymers. Generous support was provided from Dupont, Hoechst-Celanese, and the NSF National Young Investigator Program (NSF-DMR-9257569).

References and Notes

(1) Yang, H. H. *Aromatic High-Strength Fibers*; Wiley-Interscience: New York, 1989.
(2) Martin, D. C.; Thomas, E. L. *J. Mater. Sci.* **1991**, *26*, 5171–5183.
(3) Ericksen, R. H. *Polymer* **1985**, *26*, 733.
(4) Schuppert, A. A. *Makromol. Chem. Theory Simul.* **1993**, *2*, 643–651.
(5) Sweeny, W. *Journal of Polymer Science: Part A: Polymer Chemistry* **1992**, *30*, 1111–1122.
(6) Rickert, C.; Neuenschwander, P.; Suter, U. W. *Macromol. Chem.* **1994**, *195*, 511–524.
(7) Glomm, B.; Rickert, C.; Neuenschwander, P.; Suter, U. W. *Macromol. Chem.* **1994**, *195*, 525–537.
(8) Martin, D. C.; Moore, J. S.; Markoski, L. J.; Walker, K. A.; U.S. Patent No. 5,334,752, 1994.
(9) Walker, K. A.; Markoski, L. J.; Moore, J. S. *Synthesis* **1992**, 1265–68.
(10) Markoski, L. J.; Walker, K. A.; Deeter, G. A.; Spilman, G. E.; Martin, D. C.; Moore, J. S. *Chem. Mater.* **1993**, *5*, 248.
(11) Spilman, G. E.; Markoski, L. J.; Walker, K. A.; Deeter, G. A.; Martin, D. C.; Moore, J. S. *Polym. Mater. Sci. Eng.* **1993**, *68*, 139–140.
(12) Northolt, M. G. *Eur. Polym. J.* **1974**, *10*, 799–804.
(13) Haraguchi, K.; Kajiyama, T.; Takayanagi, M. *J. Appl. Polym. Sci.* **1979**, *23*, 915–926.
(14) Dobb, M. G. Strong Fibres. *Handbook of Composites*; Watt, W., Perov, B. V., Eds.; Elsevier Science Publishers: Barking, U.K., 1985; Vol. 1, Chapter 17.
(15) Jackson, C. L.; Schadt, R. J.; Gardner, K. H.; Chase, D. B.; Allen, S. R.; Gabara, V.; English, A. D. *Polymer* **1994**, *35* (6), 1123–1131.
(16) Rutledge, G. C.; Suter, U. W. *Macromolecules* **1991**, *24*, 1921–1933.

(17) Jiang, T.; Markoski, L. J.; Moore, J. S.; Martin, D. C., unpublished data.
(18) Rigney, J.; Little, M.; Martin, D. C. *J. Polym. Sci., Part B: Polym. Phys.* **1994**, *32*, 1017–1021.
(19) Martin, D. C.; Thomas, E. L. *Macromolecules* **1991**, *24*, 9.
(20) Alexander, L. E. *X-ray Diffraction Methods in Polymer Science*; Wiley-Interscience: New York, 1985.
(21) Hanna, S.; Windle, A. H. *Polymer* **1988**, *29*, 207.
(22) Biswas, A.; Blackwell, J. *Macromolecules* **1988**, *21*, 3146.
(23) Biswas, A.; Blackwell, J. *Macromolecules* **1988**, *21*, 3152.
(24) Biswas, A.; Blackwell, J. *Macromolecules* **1988**, *21*, 3158.
(25) Biswas, A. *J. Polym. Sci. Part B: Polym. Phys.* **1992**, *30*, 1375–1385.
(26) Marks, M. J. *Polym. Prep. (Am. Chem. Soc., Div. Polym. Chem.)* **1992**.
(27) McGarry, F. J.; Moalli, J. E. *Polymer* **1991**, *32* (10), 1816–1820.
(28) Lee, C. Y.-C. *Polym. Eng. Sci.* **1993**, *33*, 14.
(29) Yeh, G. S. Y.; Chen, C. J.; Boose, D. C. *Colloid Polym. Sci.* **1985**, *263*, 1–7.
(30) Chen, C. J.; Boose, D. C.; Yeh, G. S. Y. *Colloid Polym. Sci.* **1991**, *269*, 469–476.
(31) Chen, C. J.; Yeh, G. S. Y. *Colloid Polym. Sci.* **1991**, *269*, 353–363.